Available online at www.sciencedirect.com
SCIENCE DIRECT®
Journal of Magnetic Resonance 164 (2003) 145–153
JMR Journal of Magnetic Resonance
www.elsevier.com/locate/jmr

Restricted diffusion in grossly inhomogeneous fields

Lukasz J. Zielinski[a,b,*] and Pabitra N. Sen[a]

[a] *Schlumberger-Doll Research, 36 Old Quarry Road, Ridgefield, CT 06877-4108, USA*
[b] *Department of Physics, Harvard University, Cambridge, MA 02138, USA*

Received 7 March 2003; revised 28 April 2003

Abstract

We analyze the effects of geometrical restriction on the nuclear magnetization of spins diffusing in *grossly inhomogeneous fields* where radio-frequency (RF) pulses are weak relative to the total field inhomogeneity, making the rotation angle space-dependent and thus exciting multiple coherence pathways. We show how to separate the effects of restricted diffusion from the effects of the pulses in the case when the change in the field experienced by a diffusing spin in the course of the experiment is small compared to the RF magnitude. We then derive explicit formulas for the contribution of individual coherence pathways to the total magnetization in *arbitrary* pulse sequences. We find that, for long diffusion times, restriction can dramatically alter the spectrum and the shape of a particular echo, while for short times, the correction will be proportional to the pore space surface-to-volume ratio. We demonstrate these results on the example of the early echoes of the Carr–Purcell–Meiboom–Gill (CPMG) pulse sequence.

Keywords: Restricted diffusion; Inhomogeneous fields; Coherence pathways; Stray-field NMR; Off-resonance effects; CPMG

1. Introduction

Diffusion in restricted geometries and inhomogeneous magnetic fields in nuclear magnetic resonance (NMR) experiments has been extensively studied [1–11]. Most of the available literature treats the case when the field inhomogeneity is weak relative to the strength of the radio-frequency (RF) fields so that the excitation bandwidth is large and all the pulses can be assumed to be on resonance. In many systems of interest, however, the fields are *grossly* inhomogeneous and off-resonance effects become important. This is the case, for instance, for the "inside-out" NMR of well-logging [12] and materials testing [13] or for the stray-field NMR [14]. The Carr–Purcell–Meiboom–Gill (CPMG) and the steady-state free precession sequences in such systems were examined in some detail [15–18]. The rotation angle due to a given pulse varies with position, and thus every pulse generates multiple "coherence pathways," each of which contains the history of some fraction of the magnetization over the entire pulse sequence. The idea of expressing the total magnetization as a sum over the contributing coherence pathways was due to Kaiser et al. [19] who noted its usefulness for discussing the effects of pulses with arbitrary rotation angles. Following their approach, Hürlimann introduced a concise formalism for analyzing echo amplitudes and shapes for free diffusion in the presence of off-resonance pulses [16]. He found that the amount of diffusional attenuation will be different for different pathways and showed how that leads to enhanced diffusion sensitivity of the total magnetization in the CPMG. The aim of the present paper is to understand how geometrical restriction to the motion of the spins will affect the evolution of the magnetization in a system with strong off-resonance.

The effects of restriction can be very pronounced. Each coherence pathway includes spins at different local Larmor frequencies which will be differently affected by a given RF pulse. Consequently, each coherence pathway will carry a signature *spectrum* given by the product of the appropriate rotation matrix elements, each dependent on the Larmor frequency, for the pulse sequence at hand (see Section 2). Although the spectrum itself is unaffected by diffusion, its weight in the total

* Corresponding author. Fax: 1-203-438-3819.
E-mail addresses: lzielinski@ridgefield.oilfield.slb.com (L.J. Zielinski), psen@ridgefield.oilfield.slb.com (P.N. Sen).

1090-7807/$ - see front matter © 2003 Elsevier Science (USA). All rights reserved.
doi:10.1016/S1090-7807(03)00158-7

magnetization will be, with the dependence stronger for certain pathways than for others. Different sensitivity to diffusion implies different sensitivity to restriction. The spectrum of the total magnetization, then, and thus the shapes of the echoes formed, will be changed from those observed for unbounded diffusion. As we demonstrate in Section 4, this phenomenon can be quite dramatic in the long-time regime, when the spins have had ample time to sample the extent of the confinement. Since in principle every point in the spectrum contains all the information of the on-resonance measurement, a thorough understanding of the effect of restricted motion on the total spectrum could potentially allow a significant improvement in the efficiency of data acquisition [18].

Our analysis will build on a recent paper [20], where we used the Gaussian phase approximation (GPA) to formulate a general framework for computing the effects of restriction on an arbitrary coherence pathway for the case of *on-resonance* RF pulses. Here we show how the prior results can be generalized to off-resonance conditions, provided that the inhomogeneity of the field ΔB sampled by a diffusing spin in the duration t of the entire experiment is small relative to the RF field strength. This is precisely the case of interest in all the applications referred to above. We will call this condition the *small-displacement approximation*, since in most systems ΔB will scale with the average distance traversed by the spins. For diffusion in unbounded space or in a connected porous medium, for example, in a uniform gradient g, $\Delta B \sim g\sqrt{D_0 t}$, where D_0 is the diffusion coefficient of the bulk liquid. While in a suspension of oil droplets of small diameter d, $\Delta B \lesssim gd$ would remain bounded for all times, since the spin displacement would saturate at the droplet diameter. We show that in the small-displacement approximation, the effect of RF pulses will separate from the diffusional attenuation, which then can be computed independently, including any effects of restricted motion.

Our formalism is applicable to *arbitrary* pulse sequences. As an illustration, we will use it to analyze the first few CPMG echoes and show how the presence of restriction, by differentially affecting the diffusional attenuation rates of different coherence pathways, changes the total spectrum of the echo, i.e., the total contribution to the echo of spins at different Larmor frequencies.

2. Theoretical development

We follow the notation and the basic setup of [20]. To a system of spins polarized in the z-direction, diffusing in a restricted geometry in an inhomogeneous magnetic field with z-component $B(\mathbf{x},t)$, we apply an arbitrary train of N RF pulses at times $t_1, t_2, \ldots, t_N$. The spacings between the pulses are given by $\tau_k \equiv t_{k+1} - t_k$, and we let τ_N be the time measured from the Nth pulse. Total running time of the experiment from the first pulse is then $t = \sum_{k=1}^{N} \tau_k$. The RF field is given by $-2B_1 \cos(\omega_{\mathrm{RF}} t + \varphi)\,\hat{\mathbf{x}}$, where φ is the phase of the pulse, and is assumed to be uniform in space. We let ω be the offset of the local Larmor frequency from the RF frequency, $\omega \equiv -\gamma B - \omega_{\mathrm{RF}}$, and let $\omega_1 \equiv \gamma B_1$ measure the amplitude of the RF field. We then make the usual definitions:

$$\begin{aligned} m_+ &\equiv m_x + \mathrm{i}m_y, \\ m_- &\equiv m_x - \mathrm{i}m_y, \\ m_0 &\equiv m_z, \end{aligned} \tag{1}$$

where m_x, m_y, and m_z are the x, y, and z components of the magnetization. A general RF pulse acts as a rotation mixing all the magnetization components, $m_q = \sum_{q'} \Lambda_{q,q'} m_{q'}$, with $q, q' = -1, 0, +1$. Here $\Lambda_{q,q'}$ denote the rotation matrix elements that determine the fraction of the magnetization transferred from the q' to the q component. Explicit expressions for the $\Lambda_{q,q'}$ were given in [16], and we repeat them in Appendix A for the ease of reference. Here we only emphasize that under off-resonance conditions, i.e. when ω_1 cannot be assumed infinite, the $\Lambda_{q,q'}$ will depend on ω and thus on spatial location.

The evolution of the magnetization can be naturally analyzed in terms of "coherence pathways" $m_{\mathbf{q}}$, where $\mathbf{q} = \{q_0, q_1, q_2, \ldots, q_N\}$. Here q_k labels the particular magnetization component after the kth pulse, with $q_0 = 0$. We expound on the coherence pathway formalism in considerable detail in [20], while for unbounded diffusion, it is discussed in [16]. In essence, it allows the decomposition of the transverse magnetization after N pulses into a sum over all the relevant coherence pathways with the last component $q_N = +1$

$$m(\mathbf{x},t) = \sum_{\mathbf{q}} m_{\mathbf{q}}(\mathbf{x},t). \tag{2}$$

Eq. (2) sums only over the coherence pathways starting at the initial pulse. In general, if T_1-relaxation effects are significant, a fraction of the magnetization will relax between the pulses into the longitudinal direction and will form additional coherence pathway "trees" starting at each pulse. This effect can be easily incorporated into Eq. (2) (see [20]), and we leave it out here for the sake of simplicity.

Between the pulses, the spins in a given coherence pathway feel an effective field $q(t)B(\mathbf{x},t)$, where $q(t) = q_k$ for $t \in (t_k, t_{k+1})$. Their dynamics are governed by a generalization of the Torrey–Bloch equation

$$\frac{\partial}{\partial t} m_{\mathbf{q}} = \left\{ D_0 \nabla^2 - \mathrm{i}\gamma q(t) B(\mathbf{x},t) - \left(\frac{q^2(t)}{T_2} + \frac{1 - q^2(t)}{T_1} \right) \right\} m_{\mathbf{q}}, \tag{3}$$

with the partially absorbing boundary condition at the interface $D_0 \hat{\mathbf{n}} \cdot \nabla m_{\mathbf{q}} + \rho m_{\mathbf{q}} = 0$. Here D_0 is the bulk

diffusion coefficient of the liquid, ρ is the surface relaxivity, $\hat{\mathbf{n}}$ is the unit normal vector at the pore surface, and T_1 and T_2 are the longitudinal and transverse bulk relaxation times. For simplicity, we will set $\rho = 0$ throughout and so assume reflecting boundaries. We will also suppress the T_1 and T_2 relaxation effects since they can be trivially added at the end [16]. Each pulse will introduce additional inhomogeneity into the resulting magnetization via the spatially inhomogeneous $\Lambda_{q,q'}$, thus modifying the initial condition for the subsequent evolution governed by Eq. (3). In general, this would make the problem of a multiple-pulse sequence quite intractable. A simplifying approximation can be made, however, for the case of sufficiently small spin displacements.

2.1. Small-displacement approximation

We will call a displacement *small* if the corresponding change in the spin's magnetic environment is much smaller than the magnitude of the RF field. The small-displacement approximation will obtain when the average displacement of the diffusing spins is small throughout the course of the measurement. Under such conditions, we can to first order separate out the effects of the pulses and diffusion for each coherence pathway. This result, which we prove in Appendix B, hinges on the fact that, for a given flip angle, the effect of the pulses depends on the ratio of the offset frequency to the RF amplitude ω/ω_1. Thus, if a spin diffuses from some initial ω_i to $\omega_i + \delta\omega$ such that $\delta\omega/\omega_1 \ll 1$, the pulses it will feel throughout will not be much different from those at the initial offset frequency ω_i. For a uniform-gradient inhomogeneity, for example, $B(\mathbf{x}) = \mathbf{g}\cdot\mathbf{x}$, this condition requires that the width of the slice excited by each pulse be much greater than the diffusion length during the entire experiment, $B_1/g \gg \sqrt{D_0 t}$.

When the small-displacement condition is met, the magnetization in the coherence pathway $\mathbf{q}$ at a given point $\mathbf{x}$ will be weighted by the local value of the rotation matrix elements near $\mathbf{x}$. We can then write

$$m_{\mathbf{q}}(\mathbf{x},t) \simeq \left(\prod_{k=1}^{N} \Lambda_{q_k,q_{k-1}}\right)\tilde{m}_{\mathbf{q}}(\mathbf{x},t), \tag{4}$$

where $\tilde{m}_{\mathbf{q}}$ is the solution of Eq. (3) for *all* times, and *not* just between the pulses. All the matrix elements are evaluated at the same ω and depend on position via $\omega = -\gamma B(\mathbf{x}) - \omega_{\mathrm{RF}}$. We will refer to the product of the matrix elements $\prod_{k=1}^{N}\Lambda_{q_k,q_{k-1}}$ as the *spectrum* of the pathway $\mathbf{q}$. We take the initial magnetization to be uniform in space and set $\tilde{m}_{\mathbf{q}}(0) = 1$.

We note in passing that, if T_1-relaxation effects are significant, a fraction of the magnetization will relax between the pulses into the longitudinal direction and will form additional coherence pathway "trees" starting at each pulse in the sequence. For the purposes of this paper, we will ignore this extra complication. It can be easily incorporated into the general formalism by first summing over all the coherence pathways in the given tree, as in Eq. (4) for the initial pulse, and then adding up magnetizations from each tree. We explain the procedure in detail in [20]. As discussed in [16], for the CPMG pulse sequence, for example, the effects of this extra T_1 relaxation can be eliminated by the use of appropriate phase cycling.

A solution of Eq. (3) with appropriate boundary conditions, $\tilde{m}_{\mathbf{q}}$ contains *all* the diffusional attenuation information for the given coherence pathway. Since the $\Lambda_{q_k,q_{k-1}}$ are known functions of ω, the knowledge of the relevant $\tilde{m}_{\mathbf{q}}$'s and the magnetic field maps for the sample gives, via Eqs. (2) and (4), the magnetization at all times.

2.2. Solution of the generalized Torrey–Bloch equation Eq. (3)

Our approach to solving Eq. (3) will be to assume that the distribution of phases of all the spins in a pathway $\mathbf{q}$ arriving at $\mathbf{x}$ at time t, $P_{\mathbf{x},t}(\phi)$, is Gaussian. We note that this is a modification of the usual Gaussian phase approximation (GPA) where one takes the distribution of the phases of *all* the spins to be Gaussian (see, for instance, [11,20] and references therein).

In this approximation, $\tilde{m}_{\mathbf{q}}$ can be expressed in terms of the first two moments of $P_{\mathbf{x},t}(\phi)$

$$\tilde{m}_{\mathbf{q}}(\mathbf{x},t) = \exp\left\{-\mathrm{i}\langle\phi(\mathbf{x},t)\rangle_{\mathbf{q}} - \frac{\langle\phi^2(\mathbf{x},t)\rangle_{\mathbf{q}} - \langle\phi(\mathbf{x},t)\rangle_{\mathbf{q}}^2}{2}\right\}, \tag{5}$$

where

$$\begin{aligned}
\langle\phi(\mathbf{x},t)\rangle_{\mathbf{q}} &\equiv \gamma\int_0^t \mathrm{d}t_1\, q(t_1)\int \mathrm{d}\mathbf{x}'\, G(\mathbf{x},\mathbf{x}',t-t_1)B(\mathbf{x}',t_1),\\
\langle\phi^2(\mathbf{x},t)\rangle_{\mathbf{q}} &\equiv 2\gamma^2\int_0^t\int_0^{t_2}\mathrm{d}t_2\mathrm{d}t_1\, q(t_1)q(t_2)\\
&\quad\times\int \mathrm{d}\mathbf{x}'\mathrm{d}\mathbf{x}''\, G(\mathbf{x},\mathbf{x}'',t-t_2)B(\mathbf{x}'',t_2)\\
&\quad\times G(\mathbf{x}'',\mathbf{x}',t_2-t_1)B(\mathbf{x}',t_1).
\end{aligned} \tag{6}$$

The integrations extend over the total volume accessible to diffusing spins, and $G(\mathbf{x},\mathbf{x}',t)$ is the diffusion propagator satisfying $\partial_t G = D_0\nabla^2 G$ within the pore space and $D_0\hat{\mathbf{n}}\cdot\nabla G + \rho G = 0$ at the interface, with the initial condition $G(\mathbf{x},\mathbf{x}',0) = \delta(\mathbf{x}'-\mathbf{x})$. As noted above, we will consider only reflecting boundaries and thus set $\rho = 0$. The particular coherence pathway is encoded in Eq. (6) via the $q(t)$ factors.

Assuming uniform pick-up coils, the total contribution of a particular pathway to the signal measured at time t, will be given by

$$M_{\mathbf{q}}(t) = \int \mathrm{d}\mathbf{x}\, m_{\mathbf{q}}(\mathbf{x},t) = \int \mathrm{d}\mathbf{x} \left(\prod_{k=1}^{N} \Lambda_{q_k,q_{k-1}} \right) \tilde{m}_{\mathbf{q}}(\mathbf{x},t), \quad (7)$$

and the magnetization will be the sum over all the contributing pathways

$$\frac{M(t)}{M(0)} = \sum_{\mathbf{q}} M_{\mathbf{q}}(t). \quad (8)$$

The leading-order short-time behavior of $\langle \phi(\mathbf{x},t) \rangle_{\mathbf{q}}$ and $\langle \phi^2(\mathbf{x},t) \rangle_{\mathbf{q}}$ is easily computed from Eq. (6), generalizing the result in [21] to an arbitrary coherence pathway

$$\langle \phi(\mathbf{x},t) \rangle_{\mathbf{q}} = \gamma \int_0^t \mathrm{d}t'\, q(t') B(\mathbf{x},t'),$$

$$\frac{\langle \phi^2(\mathbf{x},t) \rangle_{\mathbf{q}} - \langle \phi(\mathbf{x},t) \rangle_{\mathbf{q}}^2}{2} = \gamma^2 D_0 \int_0^t \mathrm{d}t' \left(\int_0^{t'} \mathrm{d}t''\, q(t'') \nabla B(\mathbf{x},t'') \right)^2. \quad (9)$$

This formula is valid at all $\mathbf{x}$ separated by at least the diffusion length $L_{\mathrm{D}} = \sqrt{D_0 t}$ from any confining walls, and such that, near $\mathbf{x}$, the field is well-approximated by its gradient, i.e., if $|\mathbf{x} - \mathbf{x}'| < L_{\mathrm{D}}$ then $B(\mathbf{x}',t) \approx B(\mathbf{x},t) + \nabla B(\mathbf{x},t) \cdot (\mathbf{x}' - \mathbf{x})$. In fact, asymptotically for short times, Eq. (9) becomes the exact solution of Eq. (3), since the GPA is exact in that limit.

3. Application to a uniform gradient

Now we specialize to the case of a uniform-gradient field, $B(\mathbf{x},t) = \mathbf{g}(t) \cdot \mathbf{x}$, which is of particular interest in many applications.

3.1. Unbounded space

For a uniform gradient in unrestricted geometry, the formulas in Eq. (9) become exact for *all* times, giving

$$\tilde{m}_{\mathbf{q}}(\mathbf{x},t) = \exp\left\{ -\mathrm{i}\mathbf{k}_{\mathbf{q}}(t) \cdot \mathbf{x} - D_0 \int_0^t \mathrm{d}t'\, \mathbf{k}_{\mathbf{q}}^2(t') \right\}, \quad (10)$$

where

$$\mathbf{k}_{\mathbf{q}}(t) \equiv \gamma \int_0^t \mathrm{d}t'\, q(t') \mathbf{g}(t'), \quad (11)$$

is reminiscent of the $\mathbf{k}$ vector from imaging applications, but with the *effective* gradient $q(t')\mathbf{g}(t)$ in place of $\mathbf{g}(t)$. Eqs. (10) and (11) generalize to arbitrary coherence pathways the free-diffusion results of Cotts et al. [22].

If a pathway refocuses after N pulses at some time $t_{\mathbf{q}}$, then using Eq. (7), with $t > t_N$, we can write

$$M_{\mathbf{q}}(t) = A_{\mathbf{q}}^{\mathrm{free}}(t) \int \mathrm{d}\omega\, (\gamma g)^{-1} \left(\prod_{k=1}^{N} \Lambda_{q_k,q_{k-1}} \right) \mathrm{e}^{\mathrm{i}\omega(t-t_{\mathbf{q}})}, \quad (12)$$

where $g \equiv |\mathbf{g}(t)|$ and we defined the free-diffusion attenuation factor

$$A_{\mathbf{q}}^{\mathrm{free}}(t) = \exp\{-D_0 \int_0^t \mathrm{d}t'\, \mathbf{k}_{\mathbf{q}}^2(t')\}. \quad (13)$$

The reason why the attenuation factor $A_{\mathbf{q}}^{\mathrm{free}}(t)$ and the phase $\exp(\mathrm{i}\omega t)$ could be factored is that, for a uniform gradient in unbounded space, $\langle \phi^2(\mathbf{x},t) \rangle_{\mathbf{q}} - \langle \phi(\mathbf{x},t) \rangle_{\mathbf{q}}^2$ is independent of $\mathbf{x}$. This will not be the case for arbitrary field profiles or in restricted geometries since then each frequency will be weighted with a different diffusion factor. One could at this point compute $\langle \phi^2(\mathbf{x},t) \rangle_{\mathbf{q}}$ and $\langle \phi(\mathbf{x},t) \rangle_{\mathbf{q}}$ from Eq. (6) for simple closed geometries and then study the effects of restriction on individual pathways, Eq. (7), as well as the total magnetization, Eq. (8). However, we will be interested in the application to a homogeneous porous medium, where a simplification similar to that in unbounded space will take place due to the averaging over an ensemble of many pores.

3.2. Restricted geometry: homogeneous porous medium

We now consider the case of a uniform gradient $\mathbf{g}(t)$ applied across a macroscopically homogeneous medium. By "homogeneous" we mean that for the purposes of diffusion the spins in any given two-dimensional slice of the medium feel, on average, the same amount of structural confinement. More precisely, for an arbitrary choice of coordinates, we assume that the probability that a spin starting at some location in the yz plane at $x = x_1$ will diffuse in time t to some location in the yz plane at $x = x_2$, when averaged over all the initial and final positions, depends only on the separation $|x_1 - x_2|$ and not on the absolute values of x_1 and x_2. Note that this is possible even if locally the system is *not* spatially invariant.

In a homogeneous medium defined in this way, it follows that, upon averaging over the plane transverse to the gradient direction, $\langle \phi(\mathbf{x},t) \rangle_{\mathbf{q}} \to \mathbf{k}_{\mathbf{q}}(t) \cdot \mathbf{x}$, acquires the form identical to the unbounded-space result. Importantly, a similar average of $\langle \phi^2(\mathbf{x},t) \rangle_{\mathbf{q}} - \langle \phi(\mathbf{x},t) \rangle_{\mathbf{q}}^2$ will be independent of the position along the gradient, $\hat{\mathbf{g}} \cdot \mathbf{x}$. The diffusional attenuation of a particular coherence pathway, then, will be the same for all the frequencies, and thus the same as for the purely on-resonance problem. The structure of Eq. (12) will remain the same

$$M_{\mathbf{q}}(t) = A_{\mathbf{q}}(t) \int \mathrm{d}\omega\, (\gamma g)^{-1} \left(\prod_{k=1}^{N} \Lambda_{q_k,q_{k-1}} \right) \mathrm{e}^{\mathrm{i}\omega(t-t_{\mathbf{q}})}, \quad (14)$$

but with the free-diffusion attenuation factor $A_{\mathbf{q}}^{\mathrm{free}}(t)$ replaced by the general

Table 1
Normalized short-time diffusion attenuation exponents $\eta_{\mathbf{q}}$, defined in Eq. (19), for all the coherence pathways contributing to the first three CPMG echoes

Echo	Coherence pathway	$\eta^0_{\mathbf{q}}$	Exact $\alpha_{\mathbf{q}}$	Numeric $\alpha_{\mathbf{q}}$
$N=1$	$\{-+\}$	1	$\frac{32}{105\sqrt{\pi}}(2\sqrt{2}-1)$	0.314
$N=2$	$\{+-+\}$	1	$\frac{16}{105\sqrt{\pi}}(33+8\sqrt{2}-27\sqrt{3})$	0.211
	$\{-0+\}$	2	$\frac{4}{105\sqrt{\pi}}(63+4\sqrt{2}-27\sqrt{3})$	0.471
$N=3$	$\{-+-+\}$	1	$\frac{32}{315\sqrt{\pi}}(127-16\sqrt{2}+27\sqrt{3}--125\sqrt{5}+54\sqrt{6})$	0.224
	$\{+-0+\},\{+0-+\}$	$\frac{5}{3}$	$\frac{8}{525\sqrt{\pi}}(375\sqrt{5}-216\sqrt{6}--259-8\sqrt{2})$	0.336
	$\{-00+\}$	$\frac{7}{3}$	$\frac{16}{735\sqrt{\pi}}(108\sqrt{6}+63-125\sqrt{5})$	0.590
	$\{--++\}$	9	$\frac{32}{105\sqrt{\pi}}(2\sqrt{2}-1)\sqrt{3}$	0.545

$\eta^0_{\mathbf{q}}$ is the unbounded-space value and $\alpha_{\mathbf{q}}$ gives the S/V correction. + and − are a shorthand for +1 and −1, respectively, and we omitted the initial magnetization label, $q_0 = 0$, which is the same for all the pathways.

$$A_{\mathbf{q}}(t) = \exp\left\{ -\frac{\langle\phi^2(t)\rangle_{\mathbf{q}} - \langle\phi(t)\rangle^2_{\mathbf{q}}}{2} \right\}. \tag{15}$$

Here

$$\begin{aligned} \langle\phi(t)\rangle_{\mathbf{q}} &= V^{-1}\int d\mathbf{x}\,\langle\phi(\mathbf{x},t)\rangle_{\mathbf{q}}, \\ \langle\phi^2(t)\rangle_{\mathbf{q}} &= V^{-1}\int d\mathbf{x}\,\langle\phi^2(\mathbf{x},t)\rangle_{\mathbf{q}}, \end{aligned} \tag{16}$$

with V denoting the volume of the pore space. We define the *total spectrum* of an echo by $\sum_{\mathbf{q}} A_{\mathbf{q}}(t)\,(\prod_{k=1}^{N} \Lambda_{q_k,q_{k-1}})$, where the sum extends over all the contributing coherence pathways.

In the remainder of the paper, we will be interested in computing $m_{\mathbf{q}}$ at the echo time $t_{\mathbf{q}}$, where the phase $\langle\phi(t_{\mathbf{q}})\rangle_{\mathbf{q}}$ vanishes. Thus the echo-time attenuation factor will be determined entirely by $\langle\phi^2(t_{\mathbf{q}})\rangle_{\mathbf{q}}$.[1] The on-resonance case was already treated in the earlier paper [20]. Results obtained there, in light of the discussion preceding Eq. (14), will directly apply to the present problem of off-resonance conditions in a porous medium.

4. Application to CPMG in a homogeneous porous medium

We now specialize to the CPMG experiment, performed in a porous medium with a constant gradient g applied across the sample. In the presence of off-resonance conditions, it is preferable to adjust the timing between the initial 90° pulse and the first 180° pulse to optimize the signal-to-noise characteristics [23]. Thus we apply the initial 90° pulse around the x-axis at $t_1 = \omega_1^{-1}$, followed by a stream of 180° pulses around the y-axis at $t_2 = \tau$, $t_3 = 3\tau$, $t_4 = 5\tau$, etc. For simplicity, we will assume that $t_1 \ll \tau$ and thus set it to zero for the purposes of computing the diffusional attenuation. The main effect of the adjustment relevant here, therefore, will be the multiplication of the spectrum of each coherence pathway $\prod_{k=1}^{N} \Lambda_{q_k,q_{k-1}}$ by an extra factor of $\exp(-iq_1\omega/\omega_1)$. In the remainder of this section, we will consider both the short and long-time regimes and examine the effects of restriction on the total magnetization.

4.1. Short-time regime

The short-time regime will obtain when the diffusion length during τ, $L_D \equiv \sqrt{D_0\tau}$, is much shorter than the structural length scales in the medium as well as the dephasing length $L_G \equiv (D_0/\gamma g)^{1/3}$ [9,11,24,25]. The free-diffusion attenuation exponent will then acquire a pathway-dependent surface-to-volume (S/V) correction.

Explicit short-time formulas for $\langle\phi^2(t)\rangle_{\mathbf{q}}$ for an arbitrary coherence pathway at echo-formation time $t = t_{\mathbf{q}}$ were derived in [20]. We quote them in Appendix C for easy reference. As is clear from Eq. (C.4), one can always factor out of the total exponent the dimensionless combination $D_0\gamma^2 g^2\tau^3 = (L_D/L_G)^6$. We then follow [16] in introducing for each pathway $\mathbf{q}$ the diffusion attenuation exponent $\eta_{\mathbf{q}}$, normalized to be 1 for the Nth direct echo

$$\frac{2N}{3}\left(\frac{L_D}{L_G}\right)^6 \eta_{\mathbf{q}} \equiv \frac{\langle\phi^2\rangle_{\mathbf{q}}}{2}. \tag{17}$$

At echo time $t = t_{\mathbf{q}}$ the average phase $\langle\phi(t)\rangle_{\mathbf{q}}$ vanishes, and the attenuation factor in Eq. (15) becomes

$$A_{\mathbf{q}}(t_{\mathbf{q}}) = \exp\left\{ -\frac{2N}{3}\left(\frac{L_D}{L_G}\right)^6 \eta_{\mathbf{q}} \right\}. \tag{18}$$

To bring out the effects of restriction, we further write

$$\eta_{\mathbf{q}} = \eta^0_{\mathbf{q}}\left[1 - \alpha_{\mathbf{q}}\frac{L_D S}{V}\right], \tag{19}$$

where $\eta^0_{\mathbf{q}}$ is the unbounded-space attenuation exponent computed in [16] and $\alpha_{\mathbf{q}}$ determines the amount of the S/V correction. Using the formulas from Appendix C,

[1] In fact, as long as the diffusional attenuation during T_2^* can be neglected, one can set $A_{\mathbf{q}}(t) \approx A_{\mathbf{q}}(t_{\mathbf{q}})$ everywhere in Eq. (14).

we calculated $\eta_{\mathbf{q}}^0$ and $\alpha_{\mathbf{q}}$ for the pathways contributing to the first three CPMG echoes and list them in Table 1.

In unbounded space, for a given N, the direct echo pathway is characterized by the smallest $\eta_{\mathbf{q}}$ and will therefore dominate at longer times. The S/V corrections, however, are larger for the other coherence pathways, thus slowing their decay more than that of the direct echo. This trend will lead in the long-time regime to a much *faster* decay of the direct echo than of the pathways with some 0-component (longitudinal) segments. The total spectrum of the echo in the short-time regime will deviate from its unbounded-space form in Eq. (12) according to Eqs. (14) and (15), but we only show the much more dramatic effect visible in the long-time regime (see Fig. 1).

4.2. Long-time regime

The long-time regime sets in when L_{D} is the longest length in the system, longer than the structural lengths as well as the dephasing length L_{G}. Asymptotic formulas for the diffusional attenuation of an arbitrary coherence pathway in this regime were derived in [20] and we quote them in Appendix C. We note that the long-time formulas given there are valid for an *isolated* pore, while the validity of Eqs. (14) and (15) requires averaging over a homogeneous medium. In order to observe the effects described in this Section, then, one needs a system of weakly coupled pores dispersed along the whole range of off-resonance frequencies. An appropriate system would be a suspension of oil droplets, or a simple one-dimensional geometry of stacked parallel plates separated from each other with layers of diffusing fluid, like the sample used in [26].

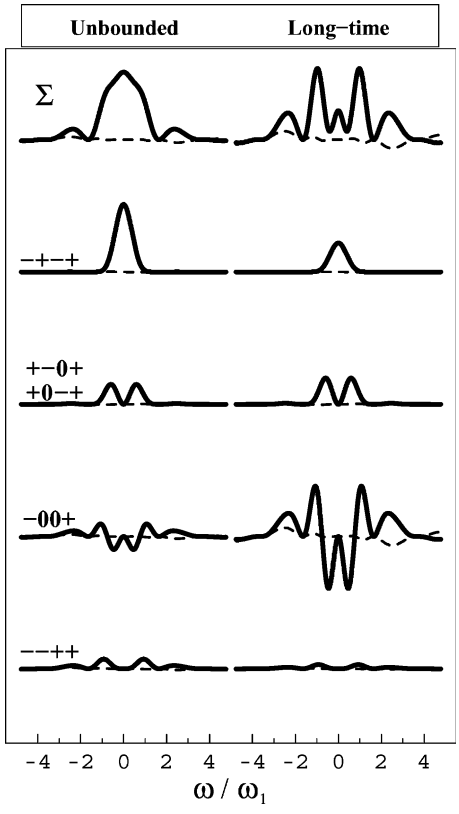

Fig. 1. The spectra of all the coherence pathways contributing to the third CPMG echo (rows 2–5) weighted with the appropriate diffusion attenuation factor, plotted as a function of the normalized offset frequency ω/ω_1. The solid line represents the y channel and the dashed line the x channel. The left column shows the unbounded-space results for the diffusion length $L_{\mathrm{D}} = 0.3L_{\mathrm{G}}$ and the right column shows the long-time regime in a one-dimensional pore of size $L_{\mathrm{S}} = L_{\mathrm{G}}$ and with $L_{\mathrm{D}} = 8.2L_{\mathrm{G}}$. The total spectra, top row, for both cases look completely different due to the altered diffusional weighting of different pathways.

For concreteness, in Fig. 1, we will consider the long-time effects of restriction on the spectrum $\sum_{\mathbf{q}} A_{\mathbf{q}}(t) \exp(-iq_1\omega/\omega_1) \prod_{k=1}^{N} \Lambda_{q_k,q_{k-1}}$ of the third CPMG echo. In addition to the direct echo, $\{0,-1,+1,-1,+1\}$, there will be four other contributing pathways: $\{0,+1,-1,0,+1\}$, $\{0,+1,0,-1,+1\}$, $\{0,-1,0,0,+1\}$, and $\{0,-1,-1,+1,+1\}$. Two of them, $\{0,+1,-1,0,+1\}$ and $\{0,+1,0,-1,+1\}$, have identical spectra and identical sensitivity to diffusion in all the regimes, so we only plot one of them, remembering that it must be double-counted when computing the complete spectrum. The echo will form at $t_{\mathbf{q}} = 6\tau$, and that is where we evaluate $A_{\mathbf{q}}(t)$.

The first column in the figure contains the results for unrestricted diffusion previously presented in [16]. Here we have used $(L_{\mathrm{D}}/L_{\mathrm{G}})^6 = 6.6 \times 10^{-5}$, small enough so that all the pathways would be visible on the same scale. Each row contains the spectrum $\prod_{k=1}^{N} \Lambda_{q_k,q_{k-1}}$ of the particular coherence pathway $\mathbf{q}$, weighted by the corresponding attenuation factor normalized by the attenuation of the direct echo, $A_{\mathbf{q}}/A_{\mathrm{CPMG}}$. The top panel shows the total spectrum. In the second column we plot the long-time regime in a one-dimensional pore of size $L_{\mathrm{S}} = L_{\mathrm{G}}$ and with the diffusion length $L_{\mathrm{D}} = 8.2L_{\mathrm{G}}$ (see Eq. (C.6)). The spectrum of each coherence pathway is fixed by the RF pulses and does not change with pulse spacings or diffusion. But the *diffusional weight* of each pathway relative to the direct echo is much different in the long-time regime, resulting in a dramatically altered total echo spectrum. The direct echo, contributing mostly to the on-resonance signal, has all but decayed away, while the dominant contribution comes from $\{0,-1,0,0,+1\}$. In general, for higher echoes, it will be the pathways with the greatest number of 0-component (longitudinal) segments that will set the attenuation characteristics, while the on-resonance contribution of the direct echo will be negligible. Incidentally, $\{0,-1,0,0,+1\}$ is nothing but the stimulated echo coherence pathway, with the prepare and read periods of duration τ and the store period of duration $\Delta = 4\tau$. We discuss its sensitivity to restricted motion for the on-resonance case in [20] in some detail.

Two further points are worth emphasizing. First, unlike in the familiar k-space imaging, the shape of the spectrum in Fig. 1 does not directly reflect any structural features of the confining space, i.e., it does not correspond to spin density in a given slice of the sample, which is uniform by the homogeneous medium assumption. Rather, it is determined by the interactions of spins at a particular Larmor frequency with the applied RF fields. And second, the fact that the peaks of the spectrum occur near $\omega/\omega_1 \approx \pm 1$ is due entirely to the particular train of RF pulses chosen, which endows the stimulated echo pathway, dominant in the long-time regime, with its spectral signature. For the usual stimulated echo sequence of three consecutive 90° pulses, the pathway $\{0,-1,0,0,+1\}$ would have a peak near $\omega/\omega_1 = 0$, and that is where the total long-time echo spectrum would have most of its weight as well.

5. Conclusion

We analyzed a macroscopically homogeneous porous medium in a grossly inhomogeneous magnetic field, where the excitation bandwidth of the RF pulses is small relative to the spread in Larmor frequencies throughout the sample. Under such conditions, each pulse necessarily excites many coherence pathways, with varying sensitivities to diffusion and hence to geometrical restriction. The resulting spectrum contains a wealth of information about the relaxation processes, and, depending on which pathways contribute, may show a much enhanced diffusion sensitivity as compared to the on-resonance behavior. The study of restricted motion in such systems is complicated by the fact that each pathway contributes differently. We developed a formalism to compute the evolution of an *arbitrary* coherence pathway for the case when the average field inhomogeneity experienced by a diffusing spin is small compared to the RF magnitude. This condition allows the separation of the effects of the pulses from diffusional attenuation. For short times, we found that restriction introduces a pathway-dependent correction to the unbounded result, proportional to the pore surface-to-volume ratio. In the long-time regime, the effects of restriction may be very pronounced, strongly changing the spectrum and the shape of a given echo. We applied our formalism to the CPMG in a grossly inhomogeneous field and showed explicitly how the inclusion of the additional coherence pathways excited by the weak RF affects the response of the system to geometrical restriction. This paper can be viewed as an extension to off-resonance pulses and restricted geometries of the work of Kaiser et al. [19] who considered a uniform-gradient field in unbounded space.

Acknowledgments

The authors would like to thank M.D. Hürlimann and Y.-Q. Song for useful discussions. Work at Harvard was partially supported by the NSF Grant DMR-99-81283.

Appendix A. RF pulse rotation matrix

In this appendix we repeat after [16] the expressions for the RF pulse matrix elements for an arbitrary frequency offset $\omega(\mathbf{x}) = -\gamma B(\mathbf{x}) - \omega_{\mathrm{RF}}$ and RF field strength $\omega_1 = \gamma B_1$. $\Omega = \sqrt{\omega_1^2 + \omega^2}$ is the total nutation frequency, t_p is the duration of the pulse and φ its phase as defined in Section 2.

$$\Lambda_{+1,+1} = \frac{1}{2}\left\{\left(\frac{\omega_1}{\Omega}\right)^2 + \left[1 + \left(\frac{\omega}{\Omega}\right)^2\right]\cos(\Omega t_p)\right\} + \mathrm{i}\left(\frac{\omega}{\Omega}\right)\sin(\Omega t_p), \tag{A.1}$$

$$\Lambda_{-1,-1} = \frac{1}{2}\left\{\left(\frac{\omega_1}{\Omega}\right)^2 + \left[1 + \left(\frac{\omega}{\Omega}\right)^2\right]\cos(\Omega t_p)\right\} - \mathrm{i}\left(\frac{\omega}{\Omega}\right)\sin(\Omega t_p), \tag{A.2}$$

$$\Lambda_{0,0} = \left(\frac{\omega}{\Omega}\right)^2 + \left(\frac{\omega_1}{\Omega}\right)^2\cos(\Omega t_p), \tag{A.3}$$

$$\Lambda_{+1,0} = \frac{\omega_1}{\Omega}\left\{\frac{\omega}{\Omega}\left[1 - \cos(\Omega t_p)\right] - \mathrm{i}\sin(\Omega t_p),\right\}e^{+\mathrm{i}\varphi} \tag{A.4}$$

$$\Lambda_{-1,0} = \frac{\omega_1}{\Omega}\left\{\frac{\omega}{\Omega}\left[1 - \cos(\Omega t_p)\right] + \mathrm{i}\sin(\Omega t_p),\right\}\mathrm{e}^{-\mathrm{i}\varphi}, \tag{A.5}$$

$$\Lambda_{0,+1} = \frac{1}{2}\frac{\omega_1}{\Omega}\left\{\frac{\omega}{\Omega}\left[1 - \cos(\Omega t_p)\right] - \mathrm{i}\sin(\Omega t_p),\right\}\mathrm{e}^{-\mathrm{i}\varphi}, \tag{A.6}$$

$$\Lambda_{0,-1} = \frac{1}{2}\frac{\omega_1}{\Omega}\left\{\frac{\omega}{\Omega}\left[1 - \cos(\Omega t_p)\right] + \mathrm{i}\sin(\Omega t_p)\right\}\mathrm{e}^{+\mathrm{i}\varphi}, \tag{A.7}$$

$$\Lambda_{+1,-1} = \frac{1}{2}\left(\frac{\omega_1}{\Omega}\right)^2\left[1 - \cos(\Omega t_p)\right]\mathrm{e}^{+\mathrm{i}2\varphi}, \tag{A.8}$$

$$\Lambda_{-1,+1} = \frac{1}{2}\left(\frac{\omega_1}{\Omega}\right)^2\left[1 - \cos(\Omega t_p)\right]\mathrm{e}^{-\mathrm{i}2\varphi}. \tag{A.9}$$

Appendix B. Separation of the effects of diffusion and off-resonance RF pulses

In this appendix we show the validity of Eq. (4) for the case of "small displacements" i.e., when the field inhomogeneity sampled by a diffusing spin is much smaller than the RF field strength. When Eq. (4) holds, the dynamics of a given coherence pathway are completely described by Eq. (3) during the entire pulse

sequence, with the effect of all the pulses well captured by applying them all together at the very end.

We examine the magnetization $m_{\mathbf{q}}$ of an individual coherence pathway, with the first pulse applied at $t_1 = 0$. Between the pulses, it evolves according to Eq. (3). Suppose that immediately after the application of the kth pulse it is equal to $m_{\mathbf{q}}(t_k^+)$. Then for $t \in (t_k, t_{k+1})$, $m_{\mathbf{q}}(t) = \mathbf{U}^{\mathbf{q}}_{t,t_k} m_{\mathbf{q}}(t_k^+)$ where $\mathbf{U}^{\mathbf{q}}_{t,t_k}$ is the pathway-dependent evolution operator formally given by $\exp\{(t-t_k) D_0\nabla^2 - \mathrm{i}\int_{t_k}^{t} \mathrm{d}t\, \gamma q(t) B\}$. Here again we suppress bulk relaxation.

Then formally, $m_{\mathbf{q}}$ after N pulses is given by

$$m_{\mathbf{q}}(t) = \mathbf{U}^{\mathbf{q}}_{t,t_N} \Lambda_{q_N,q_{N-1}} \mathbf{U}^{\mathbf{q}}_{t_N,t_{N-1}} \Lambda_{q_{N-1},q_{N-2}} \cdots \mathbf{U}^{\mathbf{q}}_{t_2,t_1} \Lambda_{q_1,q_0} m(0), \tag{B.1}$$

where the $\Lambda_{q_N,q_{N-1}}$ operator denotes multiplication by the corresponding pulse-rotation matrix element, and $m(0)$ is the initial magnetization in the z direction. We note now that for a given phase and on-resonance tip angle of the pulse, the $\Lambda_{q,q'}$ depend on the local Larmor frequency offset $\omega(\mathbf{x})$ only through the ratio $\tilde{\omega} \equiv \omega/\omega_1$. When computing $m_{\mathbf{q}}(t)$ at $\mathbf{x}$, we can expand around $\tilde{\omega} : \Lambda_{q,q'}(\tilde{\omega}') \simeq \Lambda_{q,q'}(\tilde{\omega}) + (\tilde{\omega}' - \tilde{\omega})\Lambda'_{q,q'}(\tilde{\omega}) + \cdots$. Using the fact that $\mathbf{U}^{\mathbf{q}}_{t,t_k}\mathbf{U}^{\mathbf{q}}_{t_k,t_{k-1}} = \mathbf{U}^{\mathbf{q}}_{t,t_{k-1}}$ and collecting the terms, we get, respectively, for the zeroth and first-order terms in ω_1^{-1}:

$$\begin{aligned} m^{(0)}_{\mathbf{q}}(t) &= \left(\prod_{k=1}^{N} \Lambda_{q_k,q_{k-1}}(\tilde{\omega})\right) \mathbf{U}^{\mathbf{q}}_{t,0}\, m(0) \\ &= \left(\prod_{k=1}^{N} \Lambda_{q_k,q_{k-1}}(\tilde{\omega})\right) \tilde{\boldsymbol{m}}_{\mathbf{q}}(t), \end{aligned} \tag{B.2}$$

$$m^{(1)}_{\mathbf{q}}(t) = \sum_{k=1}^{N} \Lambda_k(\tilde{\omega}) \mathbf{U}^{\mathbf{q}}_{t,t_k}(\tilde{\omega}_{k+1} - \tilde{\omega}_k) \mathbf{U}^{\mathbf{q}}_{t_k,0} m(0), \tag{B.3}$$

where we defined $\tilde{\omega}_{\mathrm{N}+1} \equiv \tilde{\omega}$ and

$$\Lambda_k(\tilde{\omega}) \equiv \frac{\Lambda'_{q_k,q_{k-1}}(\tilde{\omega})}{\Lambda_{q_k,q_{k-1}}(\tilde{\omega})} \left(\prod_{j=1}^{N} \Lambda_{q_j,q_{j-1}}(\tilde{\omega})\right). \tag{B.4}$$

Typically, $\mathbf{U}^{\mathbf{q}}_{t,t_k}(\tilde{\omega}_{k+1} - \tilde{\omega}_k)\mathbf{U}^{\mathbf{q}}_{t_k} \sim \Delta\omega_k/\omega_1$ where $\Delta\omega_k^2 \equiv \gamma^2 \langle \tau_k^{-1} \int_{t_k}^{t_{k+1}} \mathrm{d}t\, [B(\mathbf{x}_i(t)) - B(\mathbf{x}_i(0))]^2 \rangle_i$ is the ensemble average over the trajectories $\mathbf{x}_i(t)$ of all the spins. It is a measure of the average amount of field inhomogeneity experienced by a diffusing spin during the interpulse spacing τ_k. Then we have

$$m_{\mathbf{q}}(t) = \left(\prod_{k=1}^{N} \Lambda_{q_k,q_{k-1}}(\tilde{\omega})\right) \tilde{\boldsymbol{m}}_{\mathbf{q}}(t) + \mathcal{O}\left(\frac{\sum \Delta\omega_k}{\omega_1}\right). \tag{B.5}$$

For a constant gradient field, for example, $\Delta\omega_k^2 \sim \gamma^2 g^2 L_{\mathrm{D}}^2(\tau_k)$ where $L_{\mathrm{D}}^2(\tau_k) \equiv \langle [\mathbf{x}(\tau_k) - \mathbf{x}(0)]^2 \rangle$. For the CPMG in the constant gradient, then, the condition of validity of Eq. (4) is that $NL_{\mathrm{D}}(\tau)$ be much less than the thickness of the excited slice $\omega_1/\gamma g$.

Appendix C. Short and long-time on-resonance attenuation of an arbitrary coherence pathway in a uniform gradient

The following are the expressions for $\langle \phi^2(t_{\mathbf{q}}) \rangle_{\mathbf{q}}$ at echo time $t_{\mathbf{q}} = \sum_{k=1}^{N} \tau_k$ for an arbitrary coherence pathway in a uniform gradient g obtained in [20]. The setup and notation are the same as introduced in Section 2. In the GPA, $\langle \phi^2(t_{\mathbf{q}}) \rangle_{\mathbf{q}}$ determines the diffusional attenuation factor for a given pathway via Eq. (15).

$$\langle \phi^2(t_{\mathbf{q}}) \rangle_{\mathbf{q}} = \sum_{k,l=1}^{N} q_k q_l K_{kl} = \sum_{k=1}^{N} q_k^2 K_{kk} + 2\gamma^2 \sum_{k>l}^{N} q_k q_l K_{kl}, \tag{C.1}$$

where

$$K_{kk} = 2\tau_k I_1(0, \tau_k) - 2I_2(0, \tau_k), \tag{C.2}$$

and for $k \neq l$,

$$\begin{aligned} K_{kl} = {} & I_2(t_l - t_{k+1}, t_{l+1} - t_{k+1}) - [t_l - t_{k+1}] \\ & \times I_1(t_l - t_{k+1}, t_{l+1} - t_{k+1}) + \tau_l I_1(t_{l+1} - t_{k+1}, t_l - t_k) \\ & + [t_{l+1} - t_k] I_1(t_l - t_k, t_{l+1} - t_k) - I_2(t_l - t_k, t_{l+1} - t_k). \end{aligned} \tag{C.3}$$

For short times, we have

$$\begin{aligned} I_1(t', t'') = {} & -D_0\gamma^2 g^2 \frac{1}{2}\left[t''^2 - t'^2 - \frac{16}{45\sqrt{\pi}} \right. \\ & \left. \times (t''^2\sqrt{D_0 t''} - t'^2\sqrt{D_0 t'})\left(\frac{S}{V}\right)\right], \\ I_2(t', t'') = {} & -D_0\gamma^2 g^2 \frac{1}{3}\left[t''^3 - t'^3 - \frac{8}{21\sqrt{\pi}} \right. \\ & \left. \times (t''^3\sqrt{D_0 t''} - t'^3\sqrt{D_0 t'})\left(\frac{S}{V}\right)\right], \end{aligned} \tag{C.4}$$

where S/V is the surface-to-volume ratio of the pore space. The computation of $\langle \phi^2(t_{\mathbf{q}}) \rangle_{\mathbf{q}}$ becomes a simple mechanical matter of evaluating the explicit formulas for $I_1(t', t'')$ and $I_2(t', t'')$ in Eq. (C.4) at the elements of the pulse time partition defined in Section 2 according to K_{kl} and K_{kk} in Eqs. (C.3) and (C.2), and summing them up for the particular coherence pathway in Eq. (C.1). For example, for the Hahn Echo coherence pathway $\mathbf{q} = \{0, -1, +1\}$, we would have $-1/2\langle \phi^2 \rangle_{\mathrm{HE}} = 2\tau I_1(\tau, 2\tau) - 2\tau I_1(0, \tau) + 3I_2(0, \tau) - I_2(\tau, 2\tau)$, with I_1 and I_2 given in Eq. (C.4). As noted in the text, for the purposes of computing diffusional attenuation, we are neglecting the corrective shift of the first echo, assuming $\tau \gg \omega_1^{-1}$, where $\omega_1 = \gamma B_1$ measures the strength of the RF field.

In the long-time regime in a closed geometry, for an arbitrary field $B(\mathbf{x})$, Eq. (C.1) simplifies to

$$\frac{\langle \phi^2(t_{\mathbf{q}}) \rangle_{\mathbf{q}}}{2} \to \gamma^2 \left[\sum_{k=1}^{N} q_k^2 \tau_k\right] \sum_{n>0} \frac{b_n^2}{\lambda_n}, \tag{C.5}$$

where $b_n \equiv V^{-1/2}\int B(\mathbf{x})\phi_n(\mathbf{x})$ is the expansion coefficient of the magnetic field in the eigenbasis $\{\phi_n\}$ of the Laplacian operator $-D_0\nabla^2$ with reflecting boundary conditions. For the CPMG, $\tau_1 = \tau_N = \tau$, and $\tau_k = 2\tau$ for $k = 2,\ldots,N-1$. Thus the first sum in Eq. (C.5) can be written as $\sum_{k=1}^{N} q_k^2\tau_k = 2\tau(1+\sum_{k=2}^{N-1} q_k^2)$ and trivially computed for any coherence pathway. For the Nth direct CPMG echo, for example, Eq. (C.5) immediately gives $2N\tau\gamma^2\sum_{n>0} b_n^2/\lambda_n$ in agreement with [11]. In a one-dimensional box of size L_S, the sum over eigenmodes can be written in terms of integrals of $B(\mathbf{x})$, giving

$$\frac{\langle\phi^2(t_\mathbf{q})\rangle_\mathbf{q}}{2} = \frac{\gamma^2\tau}{D_0}2\left(1+\sum_{k=2}^{N-1} q_k^2\right)\left\langle\left(\int_0^x B(x')\mathrm{d}x'\right)^2\right\rangle = \frac{\gamma^2\tau g^2 L_S^4}{120 D_0}2\left(1+\sum_{k=2}^{N-1} q_k^2\right) = \frac{L_D^2 L_S^4}{60 L_G^6}\left(1+\sum_{k=2}^{N-1} q_k^2\right). \tag{C.6}$$

In the second line we evaluated the average for the case of the uniform gradient, and in the third, we cast the formula in terms of the lengths defined in Section 4.1, $L_D = \sqrt{D_0\tau}$ and $L_G = (D_0/\gamma g)^{1/3}$.

References

[1] C.H. Neuman, Spin echo of spins diffusing in a bounded medium, J. Chem. Phys. 60 (1974) 4508.

[2] K.R. Brownstein, C.E. Tarr, Importance of classsical diffusion in NMR studies of water in biological cells, Phys. Rev. A 19 (1979) 2446.

[3] J.C. Tarczon, W.P. Halperin, Interpretation of NMR diffusion measurements in uniform- and nonuniform-field profiles, Phys. Rev. B 32 (1985) 2798.

[4] P.P. Mitra, P.N. Sen, L.M. Schwartz, Short-time behavior of the diffusion coefficient as a geometrical probe of porous media, Phys. Rev. B 47 (1993) 8565.

[5] M.D. Hürlimann, K.G. Helmer, L.L. Latour, C.H. Sotak, Restricted diffusion in sedimentary rocks. Determination of surface-area-to-volume ratio and surface relaxivity, J. Magn. Reson. Ser. A 111 (1994) 169–178.

[6] R.M. Weisskoff, C.S. Zuo, J.L. Boxerman, B.R. Rosen, Microscopic susceptibility variation and transverse relaxation: theory and experiment, Magn. Reson. Med. 31 (1994) 601–610.

[7] T.M. de Swiet, P.N. Sen, Decay of nuclear magnetization by bounded diffusion in a constant field gradient, J. Chem. Phys. 100 (1994) 5597.

[8] J.E.M. Snaar, B.P. Hills, Constant gradient stimulated echo studies of diffusion in porous materials at high spectrometer fields, Magn. Reson. Imaging 15 (1997) 983–992.

[9] L.J. Zielinski, P.N. Sen, Relaxation of nuclear magnetization in a nonuniform magnetic field gradient and in restricted geometry, J. Magn. Reson. 147 (2000) 95–103.

[10] Y.-Q. Song, Detection of the high eigenmodes of spin diffusion in porous media, Phys. Rev. Lett. 85 (2000) 3878–3881.

[11] S. Axelrod, P.N. Sen, Nuclear magnetic resonance spin echoes for restricted diffusion in an inhomogeneous field: methods and asymptotic regimes, J. Chem. Phys. 114 (2001) 6878.

[12] R.L. Kleinberg, Well logging, in: Encyclopedia of Nuclear Magnetic Resonance, vol. 8, Wiley, Chichester, 1996, pp. 4960–4969.

[13] G. Eidmann, R. Savelsberg, P. Blümer, B. Blümich, The nmr mouse, a mobile universal surface explorer, J. Magn. Reson. Ser. A 122 (1996) 104–109.

[14] P.J. McDonald, Stray field magnetic resonance imaging, Prog. Nucl. Magn. Reson. Spectrosc. 30 (1997) 69–99.

[15] M.D. Hürlimann, D.D. Griffin, Spin dynamics of Carr–Purcell–Meiboom–Gill-like sequences in grossly inhomogenous b_0 and b_1 fields and application to NMR well logging, J. Magn. Reson. 143 (2000) 120–135.

[16] M.D. Hürlimann, Diffusion and relaxation effects in general stray field NMR experiments, J. Magn. Reson. 148 (2001) 367–378.

[17] Y.-Q. Song, Categories of coherences for the CPMG sequence, J. Magn. Reson. 157 (2002) 82–91.

[18] D.E. Freed, M.D. Hürlimann, U.M. Scheven, The equivalence between off-resonance and on-resonance pulse sequences and its application to steady-state free precession with diffusion in inhomogeneous fields, J. Magn. Reson. (accepted).

[19] R. Kaiser, E. Bartholdi, R.R. Ernst, Diffusion and field-gradient effects in NMR fourier spectroscopy, J. Chem. Phys. 60 (1974) 2966.

[20] L.J. Zielinski, P.N. Sen, Combined effects of diffusion, non-uniform-gradient magnetic fields, and restriction on an arbitrary coherence pathway, J. Chem. Phys. (accepted).

[21] G. Leu, X.-W. Tang, S. Peled, W.E. Maas, S. Singer, D.G. Cory, P.N. Sen, Amplitude modulation and relaxation due to diffusion in NMR experiments with a rotating sample, Chem. Phys. Lett. 332 (2000) 344–350.

[22] R.M. Cotts, M.J.R. Hoch, T. Sun, J.T. Markert, Pulsed field gradient stimulated echo methods for improved NMR diffusion measurements in hetergeneous systems, J. Magn. Reson. 83 (1989) 252–266.

[23] M.D. Hürlimann, Optimization of timing in the carr–purcell–meiboom–gill sequence, Magn. Reson. Imaging 19 (2001) 375–378.

[24] P.N. Sen, A. André, S. Axelrod, Spin echoes of nuclear magnetization diffusing in a constant magnetic field gradient and in a restricted geometry, J. Chem. Phys. 111 (1999) 6548.

[25] L.J. Zielinski, Effect of internal gradients on the NMR measurement of the surface-to-volume ratio, J. Chem. Phys. (submitted).

[26] M.D. Hürlimann, Spin echoes in a constant gradient and in the presence of simple restriction, J. Magn. Reson. Ser. A 113 (1995) 260–264.